

First-Principles Momentum-Dependent Local Ansatz Wavefunction and Momentum Distribution Function Bands of Iron

Yoshiro KAKEHASHI* and Sumal CHANDRA

*Department of Physics and Earth Sciences, Faculty of Science,
University of the Ryukyus,
1 Senbaru, Nishihara, Okinawa 903-0213, Japan*

We have developed a first-principles local ansatz wavefunction approach with momentum-dependent variational parameters on the basis of the tight-binding LDA+U Hamiltonian. The theory goes beyond the first-principles Gutzwiller approach and quantitatively describes correlated electron systems. Using the theory, we find that the momentum distribution function (MDF) bands of paramagnetic bcc Fe along high-symmetry lines show a large deviation from the Fermi-Dirac function for the d electrons with e_g symmetry and yield the momentum-dependent mass enhancement factors. The calculated average mass enhancement $m^*/m = 1.65$ is consistent with low-temperature specific heat data as well as recent angle-resolved photoemission spectroscopy (ARPES) data.

KEYWORDS: first-principles momentum-dependent local ansatz, Gutzwiller wavefunction, density functional theory, momentum distribution function, mass enhancement, electron correlations, ARPES

The quantitative description of correlated electrons in solids has been one of the central issues in condensed matter physics. Band theory has been developed towards such a quantitative description by taking into account electron-electron interactions. Density functional theory (DFT) is the state-of-the-art theory along this line. The DFT is based on the Hohenberg-Kohn theorem¹⁾ and the Kohn-Sham method.²⁾ The local density approximation (LDA) and the generalized gradient approximation (GGA) to the exchange correlation potential led to the development of the DFT as a quantitative theory.

Although the DFT has been successful for the quantitative understanding of metals and band insulators, it has failed to provide a quantitative description of more correlated electron systems such as ϵ -Fe,³⁾ Fe pnictides,⁴⁾ cuprates,⁵⁾ as well as heavy-fermion

*E-mail address: yok@sci.u-ryukyu.ac.jp, be published in J. Phys. Soc. Jpn. **85** (2016).

systems.⁹⁾ Moreover, the DFT does not describe the physical quantities such as charge and spin fluctuations, the momentum distribution function (MDF), as well as related excitations.

An alternative approach to the quantitative description of correlated electrons is to construct a first-principles effective tight-binding Hamiltonian that is compatible with the standard many-body theories and combine the Hamiltonian with them. The dynamical mean field theory (DMFT) combined with the LDA+U Hamiltonian,^{6,7)} which is equivalent to the first-principles dynamical coherent potential approximation (DCPA) that we developed,^{8,9)} is such an approach using the Green function technique and an effective medium. The theory allows us to study strongly correlated electrons within a single-site approximation.

The third approach towards the quantitative description is to combine the first-principles LDA+U Hamiltonian with the Gutzwiller variational theory.^{10,11)} The Gutzwiller wavefunction describes the ground state of correlated electrons by means of the projection operators which extract the atomic states on each atom from the Hartree-Fock state. The first-principles Gutzwiller theory can resolve a small energy difference between the states, which cannot be achieved by the LDA+DMFT.¹²⁾ Thus, the theory has been applied to many systems and has clarified the physics of electron correlations.¹¹⁾ More recently, generalized Gutzwiller density functional theory (GDFT),¹¹⁻¹³⁾ in which the wavefunction is used as a reference system to the DFT energy, has even been developed for more accurate self-consistent calculations.

The Gutzwiller wavefunction, however, does not reduce to the second-order perturbation theory in the weakly correlated limit.¹⁴⁾ Thus, it does not quantitatively describe the properties in the weakly correlated regime.

In order to overcome the difficulty in the Gutzwiller-type variational theories, we have recently proposed a momentum-dependent local ansatz (MLA) wavefunction.¹⁴⁻¹⁶⁾ The MLA is a generalization of the local ansatz approach (LA) by Fulde and Stollhoff,^{17,18)} and makes use of the Hilbert space expanded by all the two-particle excited states with the momentum-dependent variational parameters to find the best wavefunction. We demonstrated that the calculated MDF shows a distinct momentum dependence in contrast to the Gutzwiller wavefunction and calculated quasi-particle weight shows good agreement with that obtained by the DMFT combined with the numerical renormalization group technique (NRG). The MLA is therefore a new approach that is

competitive to the DMFT at zero temperature. Furthermore it allows us to calculate any static physical quantity because we know the wavefunction itself.

In this letter, we extend the MLA to the first-principles version using the LDA+U Hamiltonian. The first-principles MLA holds high momentum and total-energy resolutions because of the analytic formulation and the use of the Laplace transformation.^{15, 16)} We present the results of the first-principles MDF bands along the high-symmetry lines for bcc Fe for the first time, which are definitely not explained by the DFT or the Gutzwiller wavefunction. We demonstrate that the MDF for e_g and t_{2g} electrons are strongly momentum-dependent and thus the mass enhancement factors calculated from the jump of the MDF are also momentum-dependent. The calculated average mass enhancement is consistent with the experimental data obtained by the angle-resolved photoemission spectroscopy (ARPES) as well as those obtained from low-temperature specific heat data. Our result is also consistent with the recent result of LDA+DMFT calculations at finite temperatures, though it disagrees with the results of the first-principles Gutzwiller theory.

We start from the spd first-principles tight-binding LDA+U Hamiltonian with intraatomic Coulomb and exchange interactions between d electrons, and express it as follows assuming a system with one atom per unit cell:

$$H = H_0 + H_I . \quad (1)$$

The first term H_0 on the right-hand-side (rhs) is the Hartree-Fock Hamiltonian. The second term H_I is the residual interaction given by

$$H_I = \sum_i \left[\sum_L U_{LL} O_{iLL}^{(0)} + \sum_{(L,L')} (U_{LL'} - \frac{1}{2} J_{LL'}) O_{iLL'}^{(1)} - \sum_{(L,L')} J_{LL'} O_{iLL'}^{(2)} \right] . \quad (2)$$

Here L denotes the atomic orbitals lm on site i , \sum_L ($\sum_{(L,L')}$) expresses the sum over d ($l = 2$) orbitals (pairs between d orbitals), and $U_{LL'}$ ($J_{LL'}$) is the intraatomic Coulomb (exchange) integral between electrons on the orbitals L and L' . $O_{iLL}^{(0)}$, $O_{iLL'}^{(1)}$, and $O_{iLL'}^{(2)}$ are the intraorbital operators, the interorbital charge-charge operators, and the interorbital spin-spin operators, respectively; $O_{iLL}^{(0)} = \delta \hat{n}_{iL\uparrow} \delta \hat{n}_{iL\downarrow}$, $O_{iLL'}^{(1)} = \delta \hat{n}_{iL} \delta \hat{n}_{iL'}$, $O_{iLL'}^{(2)} = \delta \hat{\mathbf{s}}_{iL} \cdot \delta \hat{\mathbf{s}}_{iL'}$. Note that $\hat{n}_{iL\sigma} = a_{iL\sigma}^\dagger a_{iL\sigma}$, $\hat{n}_{iL} = \sum_\sigma \hat{n}_{iL\sigma}$, and $\hat{\mathbf{s}}_{iL}$ are the electron density operator for an electron with spin σ on site i and orbital L , the charge density operator, and the spin density operator, respectively. $a_{iL\sigma}^\dagger$ ($a_{iL\sigma}$) is the creation (annihilation) operator for the same electron. Furthermore $\delta \hat{n}_{iL\sigma}$, for example, should stand

for $\tilde{n}_{iL\sigma} = \langle n_{iL\sigma} \rangle_0$, $\langle \sim \rangle_0$ being the Hartree-Fock average.

In the first-principles MLA, we introduce three momentum-dependent local-ansatz operators $\tilde{O}_{iLL'}^{(\alpha)}$ ($\alpha = 0, 1, 2$) according to the residual interactions $O_{iLL'}^{(\alpha)}$:

$$\begin{aligned} \tilde{O}_{iLL'}^{(\alpha)} &= \sum_{\{kn\sigma\}} \langle k'_2 n'_2 | iL \rangle \langle iL | k_2 n_2 \rangle \langle k'_1 n'_1 | iL' \rangle \langle iL' | k_1 n_1 \rangle \\ &\quad \times \lambda_{LL'\{2'2'1'1\}}^{(\alpha)} \delta(a_{k'_2 n'_2 \sigma'_2}^\dagger a_{k_2 n_2 \sigma_2}) \delta(a_{k'_1 n'_1 \sigma'_1}^\dagger a_{k_1 n_1 \sigma_1}) . \end{aligned} \quad (3)$$

Here $a_{kn\sigma}^\dagger$ ($a_{kn\sigma}$) is the creation (annihilation) operator for an electron with momentum \mathbf{k} , band index n , and spin σ . They are given by those in the site representation as $a_{kn\sigma} = \sum_{iL} a_{iL\sigma} \langle kn | iL \rangle$, $\langle kn | iL \rangle$ being the overlap integrals.

The momentum-dependent amplitudes $\lambda_{LL'\{2'2'1'1\}}^{(\alpha)}$ in Eq. (3) are defined by

$$\lambda_{LL'\{2'2'1'1\}}^{(0)} = \eta_{L[2'2'1'1]} \delta_{LL'} \delta_{\sigma'_2 \downarrow} \delta_{\sigma_2 \downarrow} \delta_{\sigma'_1 \uparrow} \delta_{\sigma_1 \uparrow} , \quad (4)$$

$$\lambda_{LL'\{2'2'1'1\}}^{(1)} = \zeta_{LL'[2'2'1'1]}^{(\sigma_2 \sigma_1)} \delta_{\sigma'_2 \sigma_2} \delta_{\sigma'_1 \sigma_1} , \quad (5)$$

$$\lambda_{LL'\{2'2'1'1\}}^{(2)} = \sum_{\sigma} \xi_{LL'[2'2'1'1]}^{(\sigma)} \delta_{\sigma'_2 - \sigma} \delta_{\sigma_2 \sigma} \delta_{\sigma'_1 \sigma} \delta_{\sigma_1 - \sigma} + \frac{1}{2} \sigma_1 \sigma_2 \xi_{LL'[2'2'1'1]}^{(\sigma_2 \sigma_1)} \delta_{\sigma'_2 \sigma_2} \delta_{\sigma'_1 \sigma_1} . \quad (6)$$

where $\{2'2'1'1\}$ ($[2'2'1'1]$) means $\{k'_2 n'_2 \sigma'_2 k_2 n_2 \sigma_2 k'_1 n'_1 \sigma'_1 k_1 n_1 \sigma_1\}$ ($\{k'_2 n'_2 k_2 n_2 k'_1 n'_1 k_1 n_1\}$).

The η , ζ , and ξ on the rhs are variational parameters to be determined.

The operators $\tilde{O}_{iLL'}^{(0)}$, $\tilde{O}_{iLL'}^{(1)}$, and $\tilde{O}_{iLL'}^{(2)}$ describe the intraorbital correlations, the interorbital charge-charge correlations, and the interorbital spin-spin correlations, respectively. Using $\tilde{O}_{iLL'}^{(\alpha)}$ and the Hartree-Fock wavefunction $|\phi\rangle$, we construct the first-principles MLA wavefunction as follows:

$$|\Psi_{\text{MLA}}\rangle = \left[\prod_i \left(1 - \sum_L \tilde{O}_{iLL}^{(0)} - \sum_{(L,L')} \tilde{O}_{iLL'}^{(1)} - \sum_{(L,L')} \tilde{O}_{iLL'}^{(2)} \right) \right] |\phi\rangle . \quad (7)$$

The variational parameters are determined by the stationary condition for the MLA energy given by

$$E = \langle H \rangle_0 + N \epsilon_c . \quad (8)$$

Here $\langle H \rangle_0$ is the Hartree-Fock energy and N is the number of atoms in the system. The correlation energy per atom ϵ_c is obtained in the single-site approximation as follows:¹⁴⁾

$$\epsilon_c = \frac{-\langle \tilde{O}_i^\dagger \tilde{H} \rangle_0 - \langle \tilde{H} \tilde{O}_i \rangle_0 + \langle \tilde{O}_i^\dagger \tilde{H} \tilde{O}_i \rangle_0}{1 + \langle \tilde{O}_i^\dagger \tilde{O}_i \rangle_0} . \quad (9)$$

Here $\tilde{O}_i = \sum_{\alpha} \sum_{\langle LL' \rangle} \tilde{O}_{iLL'}^{(\alpha)}$ and $\tilde{H} = H - \langle H \rangle_0$, where $\sum_{\langle LL' \rangle}$ is defined by a single sum \sum_L for $L' = L$ and a pair sum $\sum_{(L,L')}$ for $L' \neq L$. Each element in Eq. (9) is calculated

with use of Wick's theorem.

We obtain self-consistent equations for the variational parameters $\lambda_{LL'\{2'2'1'1\}}^{(\alpha)}$ from the stationary condition $\delta\epsilon_c = 0$ and verify that the solution reduces to the second-order perturbation theory in the weak Coulomb interaction limit. In order to obtain an approximate but explicit solution for a more correlated regime, we adopt an additional ansatz to the variational parameters which are exact in the weak interaction limit:¹⁵⁾

$$\lambda_{LL'\{2'2'1'1\}}^{(\alpha)} = \frac{U_{LL'}^{(\alpha)} \sum_{\tau} C_{\alpha\tau\sigma'_2\sigma_2\sigma'_1\sigma_1} \tilde{\lambda}_{\alpha\tau LL'}^{(\sigma_2\sigma_1)}}{\epsilon_{k'_2 n'_2 \sigma'_2} - \epsilon_{k_2 n_2 \sigma_2} - \epsilon_{k'_1 n'_1 \sigma'_1} - \epsilon_{k_1 n_1 \sigma_1} - \epsilon_c}. \quad (10)$$

Here the Coulomb interaction energy parameters $U_{LL'}^{(\alpha)}$ are defined as $U_{LL}\delta_{LL'}$ ($\alpha = 0$), $U_{LL'} - J_{LL'}/2$ ($\alpha = 1$), and $-2J_{LL'}$ ($\alpha = 2$). The coefficients $C_{\alpha\tau\sigma'_2\sigma_2\sigma'_1\sigma_1}$ are defined by $\delta_{LL'}\delta_{\sigma'_2\downarrow}\delta_{\sigma_2\downarrow}\delta_{\sigma'_1\uparrow}\delta_{\sigma_1\uparrow}$ for $\alpha = 0$, $\delta_{\sigma'_2\sigma_2}\delta_{\sigma'_1\sigma_1}$ for $\alpha = 1$, $-(1/4)\sigma_1\sigma_2\delta_{\sigma'_2\sigma_2}\delta_{\sigma'_1\sigma_1}$ for $\alpha = 2$, $\tau = l$, and $-1/2\sum_{\sigma}\delta_{\sigma'_2-\sigma}\delta_{\sigma_2\sigma}\delta_{\sigma'_1\sigma}\delta_{\sigma_1-\sigma}$ for $\alpha = 2$, $\tau = t$. Note that l (t) denotes the longitudinal (transverse) component. We can regard the renormalization factors $\tilde{\lambda}_{\alpha\tau LL'}^{(\sigma\sigma')}$ as new variational parameters. The denominator expresses the two-particle excitation energy. Solving the self-consistent equations obtained by the variational principle $\delta\epsilon_c = 0$, we can determine these parameters.

We performed the Hartree-Fock band calculations for bcc Fe in the paramagnetic state and investigated the correlation effects using the first-principles MLA. We adopted the orbital-independent Coulomb and exchange integrals with $U_{LL} = 0.2749$ Ry, $U_{LL'} = 0.1426$ Ry, and $J_{LL'} = 0.0662$ Ry obtained by Anisimov *et al.*¹⁹⁾

Solving the Hartree-Fock equations for the tight-binding LDA+U Hamiltonian, we obtained the one-electron energy eigenvalues $\epsilon_{kn\sigma}$ for paramagnetic Fe. Figure 1 shows the energy band curves along high-symmetry lines in the first Brillouin zone. The band structure for d electrons in the Hartree-Fock approximation is similar to that obtained by the usual LDA band theory. Note that the e_g bands near the Fermi level along the $\Gamma - N - P - \Gamma$ line are much narrower than the t_{2g} ones. The other sp bands are mostly far from the Fermi level (ϵ_F); thus the Fermi surface of Fe is mainly determined by the d bands.

The MDF in the first-principles MLA is given by

$$\langle n_{kn\sigma} \rangle = f(\tilde{\epsilon}_{kn\sigma}) + \frac{N \langle \tilde{O}_i^\dagger \tilde{n}_{kn\sigma} \tilde{O}_i \rangle_0}{1 + \langle \tilde{O}_i^\dagger \tilde{O}_i \rangle_0}. \quad (11)$$

The first term on the rhs is the Fermi-Dirac distribution function for the Hartree-Fock independent electrons. $\tilde{\epsilon}_{kn\sigma}$ denotes the energy eigenvalue measured from ϵ_F . The second

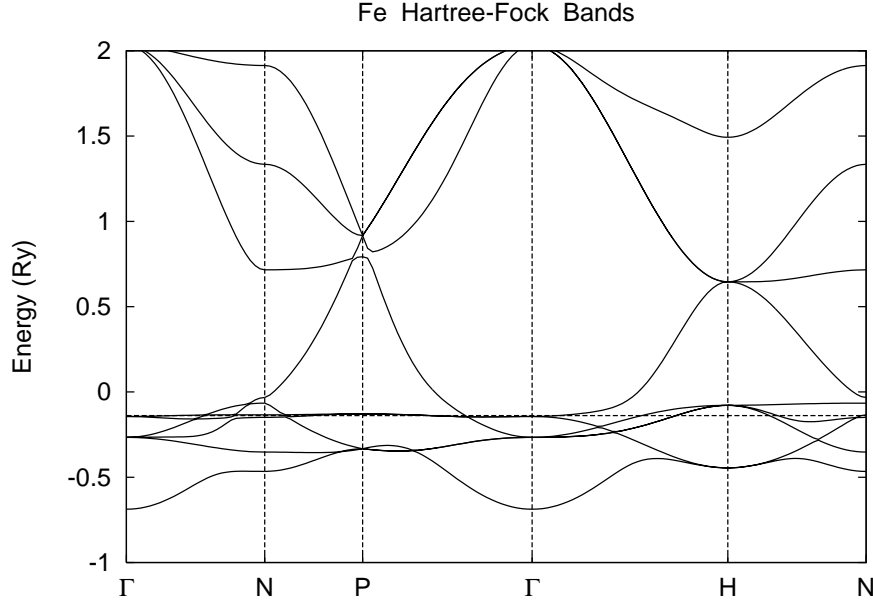


Fig. 1. Hartree-Fock one-electron energy bands of bcc Fe along high-symmetry lines of the first Brillouin zone. The Fermi level (-0.1387 Ry) is expressed by the horizontal dashed line.

term is the correlation correction. Its numerator is expressed in the paramagnetic state as

$$N\langle\tilde{O}_i^\dagger\tilde{n}_{kn\sigma}\tilde{O}_i\rangle_0 = \sum_{\alpha\tau\langle LL'\rangle} q_{\alpha\tau}U_{LL'}^{(\alpha)2}\tilde{\lambda}_{\alpha\tau LL'}^2(\bar{B}_{LL'n}(\mathbf{k})f(-\tilde{\epsilon}_{kn\sigma}) - \bar{C}_{LL'n}(\mathbf{k})f(\tilde{\epsilon}_{kn\sigma})). \quad (12)$$

Here $q_{\alpha\tau}$ is a numerical factor taking the value of 1 for $\alpha = 0$, 2 for $\alpha = 1$, $1/8$ for $\alpha = 2, \tau = l$, and $1/4$ for $\alpha = 2, \tau = t$. Note that there is no spin dependence in the variational parameters $\tilde{\lambda}_{\alpha\tau LL'}$ in the paramagnetic state. $\bar{B}_{LL'n}(\mathbf{k})$ is a momentum-dependent particle contribution above ϵ_F given by $\bar{B}_{LL'n}(\mathbf{k}) = |u_{Ln}(\mathbf{k})|^2 B_{L'Ln}(\epsilon_{kn\sigma}) + |u_{L'n}(\mathbf{k})|^2 B_{LL'n}(\epsilon_{kn\sigma})$. The hole contribution $\bar{C}_{LL'n}(\mathbf{k})$ is defined by $\bar{B}_{LL'n}(\mathbf{k})$ in which $B_{LL'n}(\epsilon_{kn\sigma})$ has been replaced by $C_{LL'n}(\epsilon_{kn\sigma})$. The energy-dependent functions $B_{LL'n}(\epsilon_{kn\sigma})$ and $C_{LL'n}(\epsilon_{kn\sigma})$ are given by the Laplace transforms of the local density of states in the Hartree-Fock approximations and have been given in the Appendix in Ref. 15 for the single-orbital case. Note that the MDF in the first-principles MLA depends on the momentum \mathbf{k} not only via the energy $\epsilon_{kn\sigma}$ but also via $u_{Ln}(\mathbf{k})$, *i.e.*, the eigenvector at each \mathbf{k} point.

We have calculated the MDF in paramagnetic Fe using Eq. (11). Figure 2 shows the result along high-symmetry lines. (Note that the wavevector \mathbf{k} is measured in the unit

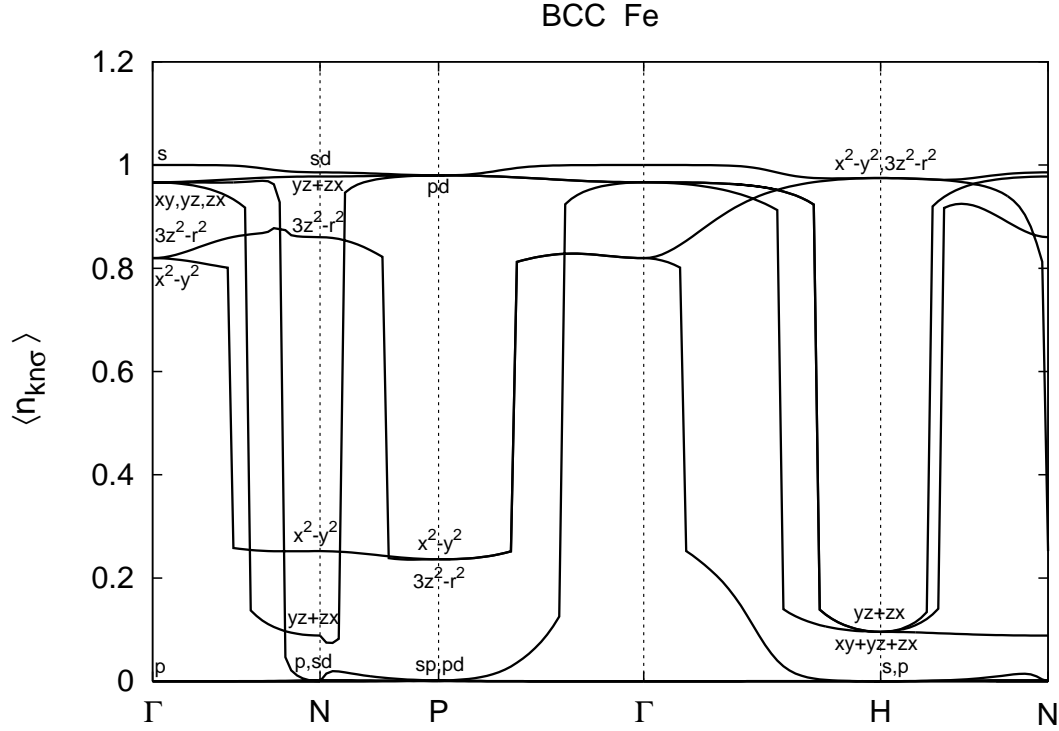


Fig. 2. Momentum distribution functions ($\langle n_{k_n\sigma} \rangle$) along high-symmetry lines for bcc Fe. Orbital symmetry functions and their hybridized states for the branches at high-symmetry points are written in the figure.

of $2\pi/a$, a being the lattice constant.) We find strong momentum dependence of $\langle n_{k_n\sigma} \rangle$ along the lines, which is not described by the Hartree-Fock wavefunction.

At point Γ , we have a free-electron-like MDF $\langle n_{k_n\sigma} \rangle = 1.00$ for s electrons with the Hartree-Fock one-electron energy $\epsilon_{k_n\sigma} = -0.69$ Ry ($< \epsilon_F$) (see Fig. 1), while we have the MDF $\langle n_{k_n\sigma} \rangle = 0.97$ for d electrons with t_{2g} symmetry, which are associated with the Hartree-Fock one-electron energy $\epsilon_{k_n\sigma} = -0.27$ Ry ($< \epsilon_F$), and the MDF $\langle n_{k_n\sigma} \rangle = 0.82$ for d electrons with e_g symmetry with the energy $\epsilon_{k_n\sigma} = -0.14$ Ry ($< \epsilon_F$) in Fig. 1. For the p electrons associated with the energy $\epsilon_{k_n\sigma} = 2.03$ Ry ($> \epsilon_F$), we again have a free-electron-like MDF $\langle n_{k_n\sigma} \rangle = 0.00$.

When the momentum \mathbf{k} moves toward point N along the Γ -N line, the MDF for t_{2g} electrons splits into three branches. The first branch is almost constant and has a value $\langle n_{k_n\sigma} \rangle = 0.98$ at point N. The second branch jumps down at $\mathbf{k}_F = (0.39, 0.39, 0.00)$ on the Fermi surface and approaches $\langle n_{k_n\sigma} \rangle = 0.00$ at point N. The third branch decreases with the change in \mathbf{k} toward point N, jumps down at $\mathbf{k}_F = (0.28, 0.28, 0.00)$,

Table I. Mass enhancement factors for e_g electrons at various wavevectors \mathbf{k} on the Fermi surface.

\mathbf{k}	(0.23, 0.23, 0.00)	(0.50, 0.50, 0.28)	(0.32, 0.32, 0.32)	(0.00, 0.17, 0.00)
m_{kn}^*/m	1.84	1.71	1.78	1.82

and approaches $\langle n_{kn\sigma} \rangle = 0.088$ at point N. The MDF for e_g electrons splits into two branches. The branch with $3z^2 - r^2$ symmetry increases and approaches to $\langle n_{kn\sigma} \rangle = 0.86$ at point N. The second branch with $x^2 - y^2$ symmetry decreases along the Γ -N lines, jumps down at $\mathbf{k}_F = (0.23, 0.23, 0.00)$, and approaches $\langle n_{kn\sigma} \rangle = 0.25$ at point N. The s electron branch of the MDF hardly changes and approaches to the value $\langle n_{kn\sigma} \rangle = 0.99$ at point N. The p electron branch also shows flat behavior with $\langle n_{kn\sigma} \rangle = 0.00$ because there is no hybridization with d electrons and their one-electron energies are far above the Fermi level (see Fig. 1).

The basic behavior of the MDF for s , p , and d electrons mentioned above is also seen on the other high-symmetry N-P, P- Γ , Γ -H, and H-N lines. We find that the MDF branches associated with e_g electrons show large deviations from 0 and 1, indicating strong electron correlations. The MDF associated with t_{2g} electrons also shows significant deviations from 0 and 1. On the other hand, the s - and p -like MDFs have values close to 1 or 0, indicating that the independent electron band picture is applicable to their electrons.

The jump of the MDF on the Fermi surface gives the quasi-particle weight Z_{kn} or the inverse mass enhancement factor $(m_{nk}^*/m)^{-1}$ according to the Fermi liquid theory. Since the hybridization between the sp and d electrons excludes the sp -like bands near the Fermi level, most of the Fermi surface of the bcc Fe is formed by the d bands. The mass enhancement factors for e_g and t_{2g} electrons calculated along high-symmetry lines are presented in Tables I and II, respectively. We find that the mass enhancements for e_g electrons are momentum-dependent and show considerably large values of $m_{nk}^*/m = 1.71 - 1.84$, because these electrons form narrow bands near the Fermi level. The t_{2g} electrons yield smaller enhancements of $m_{nk}^*/m = 1.14 - 1.29$.

We have calculated the averaged mass enhancement factor over the Fermi surface and obtained $m^*/m = 1.648$. This value is consistent with the experimental data of $m^*/m = 1.4 - 2.1$ obtained from the low-temperature specific heat.²⁰⁻²²⁾ Our result also agrees well with the recent result of $m^*/m = 1.7$ obtained by an ARPES experiment.²³⁾

Table II. Mass enhancement factors for t_{2g} electrons at various wavevectors \mathbf{k} on the Fermi surface.

\mathbf{k}	(0.28, 0.28, 0.00)	(0.39, 0.39, 0.00)	(0.50, 0.50, 0.09)	(0.20, 0.20, 0.20)
$m_{\mathbf{k}n}^*/m$	1.28	1.14	1.16	1.25
\mathbf{k}	(0.00, 0.58, 0.00)	(0.00, 0.73, 0.00)	(0.15, 0.85, 0.00)	(0.18, 0.82, 0.00)
$m_{\mathbf{k}n}^*/m$	1.29	1.27	1.27	1.29

In order to examine the dependence of m^*/m on the Coulomb integrals, we performed the same calculations using the alternative set $U_{LL} = 0.3233$ Ry, $U_{LL'} = 0.1932$ Ry, and $J_{LL'} = 0.0650$ Ry, which was adopted in our LDA+DCPA calculations.²⁴⁾ We obtained $m^*/m = 1.551$, a deviation of only 6% from the value of 1.648. We also suggest that the ferromagnetic spin polarization may reduce the mass enhancement by about 5% because of the change in the weight between e_g and t_{2g} electrons on the Fermi surface.

The effective mass of Fe has recently been much investigated from the quantitative viewpoint. Sánchez-Barriga *et al.*²³⁾ performed the three-body theory + LDA-DMFT calculations and obtained $m^*/m = 1.25$ on the Γ -N line, which is too small as compared with the ARPES result of $m^*/m = 1.7$. Katanin *et al.*²⁵⁾ reported the results of LDA+DMFT calculations using the quantum Monte-Carlo technique (QMC) at 1000 K. They obtained $m_{t_{2g}}^*/m = 1.163$ for t_{2g} electrons, in agreement with our result of $m_{t_{2g}}^*/m \approx 1.2$. However, the value for e_g electrons was not obtained because of the non-Fermi liquid behavior due to strong fluctuations in the narrow e_g bands at finite temperatures. More recently, Pourovskii *et al.*³⁾ reported the LDA+DMFT calculations for bcc Fe using the continuous-time QMC at 300 K. They obtained $m^*/m \approx 1.577$. The latter is consistent with the present result of $m^*/m = 1.648$.

First-principles Gutzwiller theory underestimates the mass enhancement factor. The LDA+Gutzwiller calculations¹³⁾ yield a reasonable value of $m^*/m \approx 1.564$, but a too large Coulomb interaction parameter of $\bar{U} = 7.0$ eV was adopted there. More recent calculations based on the LDA+Gutzwiller theory with reasonable values of $\bar{U} = 2.5$ eV and $\bar{J} = 1.2$ eV result in $m_{e_g}^*/m \approx 1.08$ for e_g electrons and $m_{t_{2g}}^*/m \approx 1.05$ for t_{2g} electrons,²⁶⁾ which are too small as compared with the ARPES value of $m^*/m = 1.7$.

In summary, we have developed a first-principles MLA on the basis of the tight-binding LDA+U Hamiltonian with intra-atomic Coulomb and exchange interactions. The first-principles MLA reduces to the Rayleigh-Schrödinger perturbation theory in

~~the weakly correlated limit, as it should, and quantitatively describes the correlated~~
electron state with use of the self-consistent momentum-dependent variational parameters.

We obtained the first-principles MDF bands for bcc Fe along high-symmetry lines, and clarified the band structure of the MDF for s , p , and d electrons for the first time. We found a large deviation from the Fermi-Dirac distribution function for the branches associated with e_g and t_{2g} electrons, while the sp electron branches follow the usual band theory. We obtained the momentum-dependent mass enhancement factors $m_{k_n}^*/m$ along the high-symmetry line for the first time. We found the mass enhancements of $m_{e_g}^*/m \approx 1.8$ for e_g electrons and $m_{t_{2g}}^*/m \approx 1.2$ for t_{2g} electrons, and an average mass enhancement of $m^*/m = 1.648$. This result explains the recent ARPES value of 1.7 and the data obtained from the low-temperature specific heat. It is also consistent with the theoretical result of 1.577 at 300 K based on the recent LDA+DMFT calculations. First-principles Gutzwiller theory underestimates the mass enhancement of bcc Fe by 35% . For the quantitative description of bcc Fe, the momentum dependence of the variational parameters is essential. The present calculations have been performed in the paramagnetic state. In order to discuss more quantitative aspects of the theory, we have to perform ferromagnetic calculations. Systematic investigations of the ferromagnetic Fe, Co, and Ni using the first-principles MLA are left for future work.

The present work was supported by a Grant-in-Aid for Scientific Research (25400404).

References

- 1) P. Hohenberg and W. Kohn, Phys. Rev. **136**, B864 (1964).
- 2) W. Kohn and L. J. Sham, Phys. Rev. **140**, A1133 (1965).
- 3) L. V. Pourovskii, J. Mravlje, M. Ferrero, O. Parcollet, and I. A. Abrikosov, Phys. Rev. B **90**, 155120 (2014).
- 4) M. Imada and T. Miyake, J. Phys. Soc. Jpn. **79**, 112001 (2010).
- 5) See, for example, P. Fulde, *Correlated Electrons in Quantum Matter* (World Scientific, Singapore, 2012).
- 6) G. Kotliar, S. Y. Savrasov, K. Haule, V. S. Oudovenko, O. Parcollet, and C. A. Marianetti, Rev. Mod. Phys. **78**, 865 (2006).
- 7) V. I. Anisimov and Yu. A. Izyumov, *Electronic Structure of Strongly Correlated Materials* (Springer, Berlin, 2010).
- 8) Y. Kakehashi and M. A. R. Patoary, J. Phys. Soc. Jpn. **80**, 034706 (2011).
- 9) Y. Kakehashi, *Modern Theory of Magnetism in Metals and Alloys* (Springer Verlag Pub., Berlin, 2013) Chap. 3.
- 10) J. Bünemann, F. Gebhard, and W. Weber, Found. of Phys. **30**, 2011 (2000).
- 11) J. Bünemann, arXiv:1207.6456 [cond-mat.str-el] (2012).
- 12) T. Schickling, F. Gebhard, J. Bünemann, L. Boeri, O. K. Andersen, and W. Weber, Phys. Rev. Lett. **108**, 036406 (2012).
- 13) X. Y. Deng, L. Wang, X. Dai, and Z. Fang, Phys. Rev. B **79**, 075114 (2009).
- 14) Y. Kakehashi, T. Shimabukuro, and C. Yasuda, J. Phys. Soc. Jpn. **77**, 114702 (2008).
- 15) M. Atiqur R. Patoary and Y. Kakehashi, J. Phys. Soc. Jpn. **80**, 114708 (2011).
- 16) M. Atiqur R. Patoary and Y. Kakehashi, J. Phys. Soc. Jpn. **82**, 013701 (2013); **82**, 084710 (2013).
- 17) G. Stollhoff and P. Fulde, Z. Phys. B **26**, 257 (1977); **29**, 231 (1978).
- 18) A. M. Oleś and G. Stollhoff, Phys. Rev. B **29**, 314 (1984).
- 19) V. I. Anisimov, F. Aryasetiawan, and A. I. Lichtenstein, J. Phys: Condens. Matter **9**, 767 (1997).
- 20) C. H. Cheng, C. T. Wei, and P. A. Beck, Phys. Rev. **120**, 426 (1960).
- 21) H. Cho and M. Scheffler, Phys. Rev. B **53**, 10685 (1996).

- ~~22) L. Chioncel, L. Vitos, I. A. Abrikosov, J. Kollár, M. I. Katsnelson, and A. I. Lichtenstein, Phys. Rev. B **67**, 235106 (2003).~~
- 23) J. Sánchez-Barriga, J. Fink, V. Boni, I. Di Marco, J. Braun, J. Minár, A. Varykhalov, O. Rader, V. Bellini, F. Manghi, H. Ebert, M. I. Katsnelson, A. I. Lichtenstein, O. Eriksson, W. Eberhardt, and H. A. Dürr, Phys. Rev. Lett. **103**, 26720 (2009).
- 24) Y. Kakehashi, , M. Atiqur R. Patoary, and T. Tamashiro, Phys. Rev. B **81**, 245133 (2010).
- 25) A. A. Katanin, A. I. Poteryaev, A. V. Efremov, A. O. Shorikov, S. L. Skornyakov, M. A. Korotin, and V. I. Anisimov, Phys. Rev. B **81**, 045117 (2010).
- 26) Giovanni Borghi, Michele Fabrizio, and Erio Tosatti, Phys. Rev. B **90**, 125102 (2014).